

Synthesis and photophysics of platinum capped phenylene ethynylene oligomers

Julia M. Keller,[†] Abigail H. Shelton,[†] Randi S. Price,[†] Naresh Duvva,[‡] and Kirk S. Schanze^{*†,‡}

[‡]Department of Chemistry, University of Texas at San Antonio, San Antonio, TX 78249

[†]Department of Chemistry, University of Florida, PO Box 117200, Gainesville, Florida 32611

Email: kirk.schanze@utsa.edu

This article is dedicated to the memory Alan R. Katritzky who was my colleague in the Department of Chemistry, Organic Chemistry Division, University of Florida, from 1986 – 2014.

Received mm-dd-yyyy

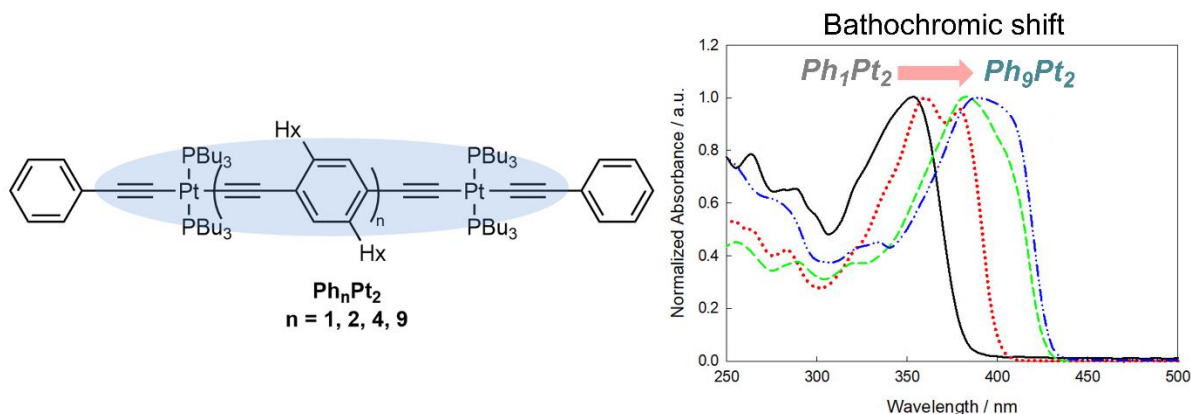
Accepted mm-dd-yyyy

Published on line mm-dd-yyyy

Dates to be inserted by editorial office

Abstract

A series of dinuclear platinum-acetylide oligomers Ph_nPt_2 were synthesized, consisting of alkylated phenylene ethynylene oligomers of varying lengths ($n = 1, 2, 4$ and 9) capped by *trans*-bis(tributylphosphine)(2-phenylethynyl)-platinum(II) end groups. The oligomers were designed to examine the effects on the excited state properties between two platinum moieties of increasing organic spacer distances. Optical data conclude that the ground state and singlet exciton remain delocalized throughout the series, but approaching its limit. The extent of delocalization in the triplet exciton is reached by Ph_4Pt_2 , and phosphorescence yields at ambient temperatures decreased with increasing spacer length until phosphorescence emission was almost elusive in the $n = 9$ oligomer. Lifetime trends of the singlet and triplet excited states correlate well with the decreasing percent heavy metal character as the organic spacer is lengthened.



Keywords: Platinum acetylide, phenylene ethynylene oligomers, triplet state, phosphorescence

Introduction

There have been a range of platinum acetylide structures reported in the literature,¹⁻⁴ including oligomers, polymers, and dendrimers, used for many different optical and electronic applications⁵⁻¹² owing to the unique photophysical properties^{2,4,13-16} of these materials. In general, the key aspect toward the advancement of materials applications is to define distinct relationships between chemical structure and spectroscopic properties.¹⁶⁻¹⁹ The nature of the structure-property relationship is also fundamentally important in understanding the interaction of light with matter and the information that can be elicited from experiments. One such issue is the relationship between structure and the delocalization of the singlet and triplet excitons.^{20,21}

Our group has studied delocalization of the singlet and triplet states of platinum acetylide oligomers.^{13,22-28} It was found that ground state absorbance and fluorescence properties are dependent on the conjugation length of the material, as these states are defined as being delocalized through the metal-organic π -conjugated electron system. The triplet state, however, was concluded to be spatially confined, as the properties of this state change very little in relation to changes in the length of the Pt-acetylide oligomer.

Most of the studies investigating extended π -conjugation in the organic ligands of platinum acetylide oligomers focus on a single platinum atom and various ligands, or oligomers and polymers with identical repeat units; the understanding of delocalization in excited states is therefore limited. One example of such is a set of studies reported by Cooper and Rogers, *et al.*²⁹⁻³⁵ Symmetrically substituted, mono-substituted, and asymmetrically substituted platinum acetylides were investigated and compared to the analogous organic butadienes. For the symmetrically substituted materials,²⁹ increased π -conjugation gave rise to a red shifting

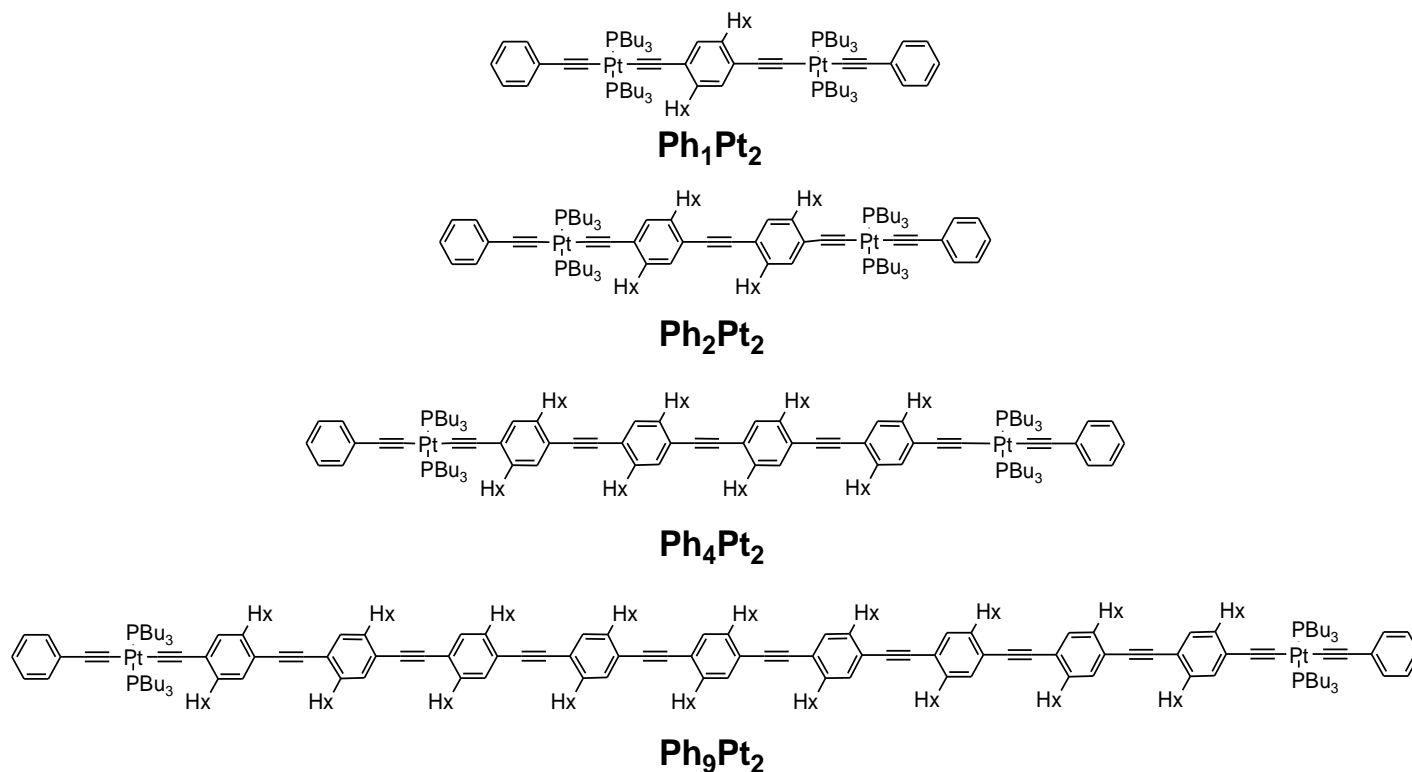


Chart 1. Structures of platinum-capped phenylene ethynylene oligomers

of the S_0 - S_1 and T_1 - T_n transitions. It was also concluded that the spin-orbit coupling effect of platinum on the ground and excited-state properties is reduced with increased conjugation length because the S_0 - S_1 transition is more localized on the ligand. As the ligand size increased, the transition takes on more $^1\pi\pi^*$ character, therefore decreasing the mixing with orbitals localized on the platinum center. For the asymmetrically substituted complexes,³⁵ absorption and emission data showed evidence of singlet exciton delocalization across the central platinum atom. The phosphorescence from the asymmetric complexes always arises from the largest ligand, verifying Kasha's Rule in that the triplet exciton migrates towards the lowest energy ligand. Comparison of these complexes with the mono-substituted compounds³³ concluded that while the singlet exciton was delocalized through the platinum atom, the excited triplet states of each analogous compound were nearly identical, implying that the triplet exciton is confined to the larger organic ligand.

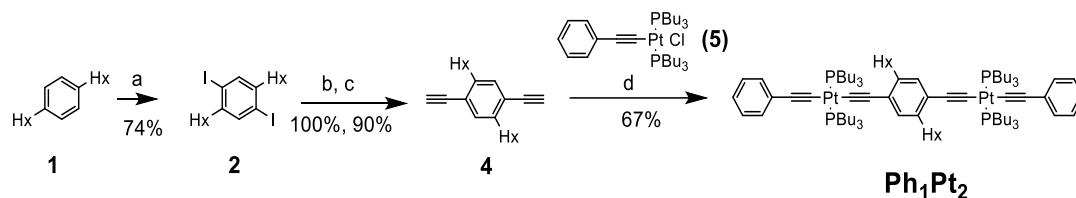
The current study aims to examine effects of ground state and excited state delocalization between two platinum centers as the length of a π -conjugated spacer is extended. The spacer to be studied is a series of oligo(phenylene ethynylene)s that feature platinum end-caps (Ph_nPt_2 , Chart 1). The synthesis and photophysical analysis of oligo(phenylene ethynylene)s (OPEs) lacking Pt-acetylide end caps was previously reported by Godt and co-workers.³⁶ Their work showed that increase of the OPE length resulted in a bathochromic shift of the ground state absorption and fluorescence emission maxima. A unique feature of the oligomers was the distinctive structure of the absorption and emission band, believed to be due to vibronically distinct electronic transitions.

Results and Discussion

Synthesis. The general synthesis of the Ph_nPt_2 series was modeled after the synthesis of monodisperse oligo(para-phenylene ethynylene)s (OPEs), reported by Godt and coworkers.³⁶ The strategy involved a divergent-convergent synthesis starting from 1,4-dihexyl-2-(3-hydroxyprop-1-ynyl)-5-[2-(triisopropylsilyl)ethynyl]benzene (**7**, Scheme S-2) in Pd/Cu-catalyzed alkyne-aryl couplings. The orthogonal acetylene protecting groups hydroxymethyl (HOM) and triisopropylsilyl (TIPS) were used to construct various smaller synthons that could be selectively deprotected and reacted, as well as to facilitate purification processes. The incorporation of the alkylated phenyl moieties is advantageous as well, as the hexyl (Hx) groups provide solubility in typical organic solvents. Deprotection of either the HOM or TIPS protecting group (one at a time) of the final OPE synthons affords a stable terminal acetylene that can be reacted with a mono-substituted Pt(II) endcap, via Hagihara conditions, to afford the analogous platinum acetylides of the series, Ph_nPt_2 (Chart 1).

The synthesis of Ph_1Pt_2 is outlined in Scheme 1. A copious amount of the main starting material, **2**, was initially prepared (~ 50 g). Iodination of known compound **1** proved to be a challenge, as following standard literature procedures gave irreproducible results from reaction to reaction. A reproducible yield of **2** was finally achieved when acetic anhydride was used in the reaction with both acetic acid and sulfuric acid, rather than the use of water as a co-solvent.³⁸

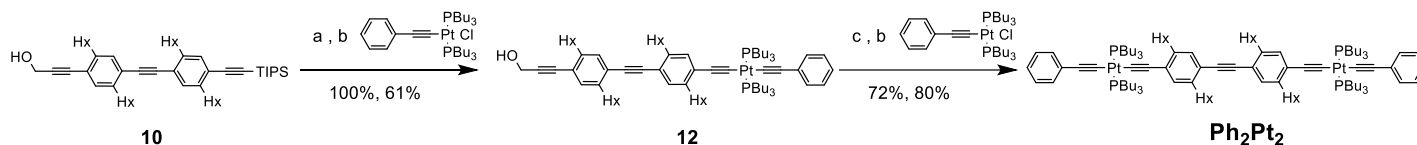
Subsequent coupling of **2** with two equivalents of TMS-acetylene afforded the symmetrically-protected intermediate (**3**, Scheme S-1) in a high yield; deprotection of this intermediate gave **4**. Copper-catalyzed Hagihara coupling with 2 equivalents of endcap **5** yielded oligomer Ph_1Pt_2 as a yellow solid, in 51% overall yield.



a) $I_2/NaIO_4$, H_2SO_4 , $AcOH/Ac_2O$; b) TMS-acetylene, $Pd(PPh_3)_2Cl_2/CuI$, THF/ iPr_2NH , $70^\circ C$, 12h; c) TBAF, THF, rt, dark, 2h; d) CuI , THF/ Et_2NH , rt, 1.5h.

Scheme 1. Synthesis of Ph_1Pt_2

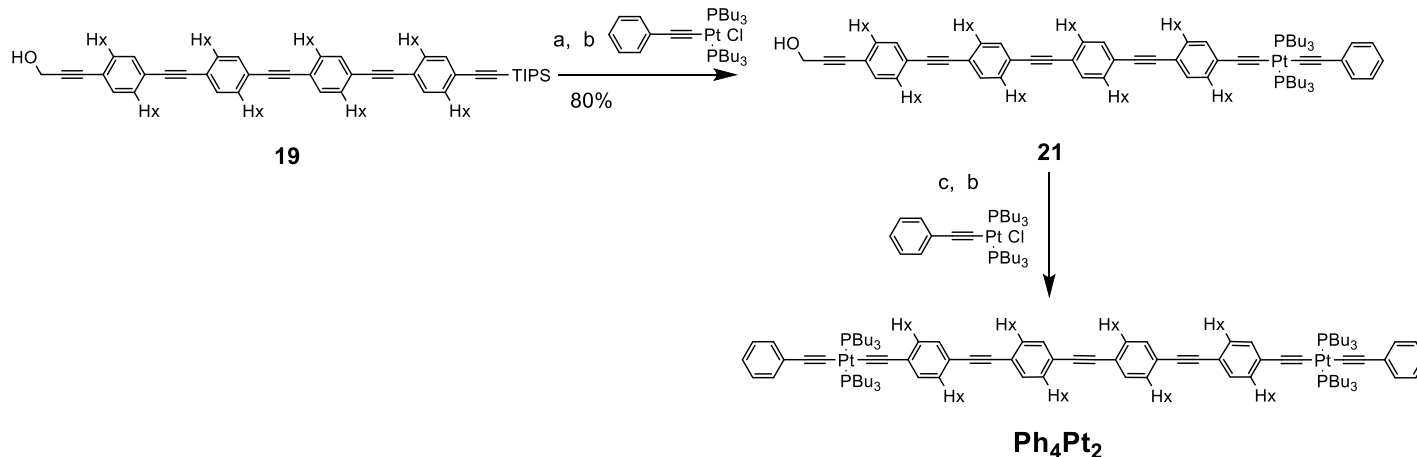
Construction of the longer oligomers required the use of orthogonal protecting groups, as discussed previously. Coupling and selective deprotection of the HOM and TIPS protecting groups afforded the orthogonally-protected dimer **10** (Scheme S-2) as previously reported by Godt *et al.*³⁶ Stepwise deprotection/Hagihara couplings with *trans*-(PhCC)Pt(PBu₃)₂Cl (**5**) to each end of the oligomer afforded Ph_2Pt_2 as a yellow solid in 30% yield (Scheme 2).



a) TBAF, THF, rt, 2h; b) $Pd(PPh_3)_2Cl_2/CuI$, THF/piperidine, $50^\circ C$, 12h; c) MnO_2/KOH , ether, rt, dark, 12h;

Scheme 2. Synthesis of Ph_2Pt_2

The synthesis of Ph_4Pt_2 was carried out in a similar manner (Scheme 3). Preparation of the orthogonally-protected tetramer **19** (Scheme S-3) was previously described.³⁶ Again, stepwise deprotection/Hagihara couplings of each acetylene unit with *trans*-(PhCC)Pt(PBu₃)₂Cl (**5**) afforded Ph_4Pt_2 in 72% yield.



a) TBAF, THF, rt, 2h; b) CuI , THF/ $NHEt_2$, rt, 4h; c) MnO_2/KOH , ether, rt, dark, 4h.

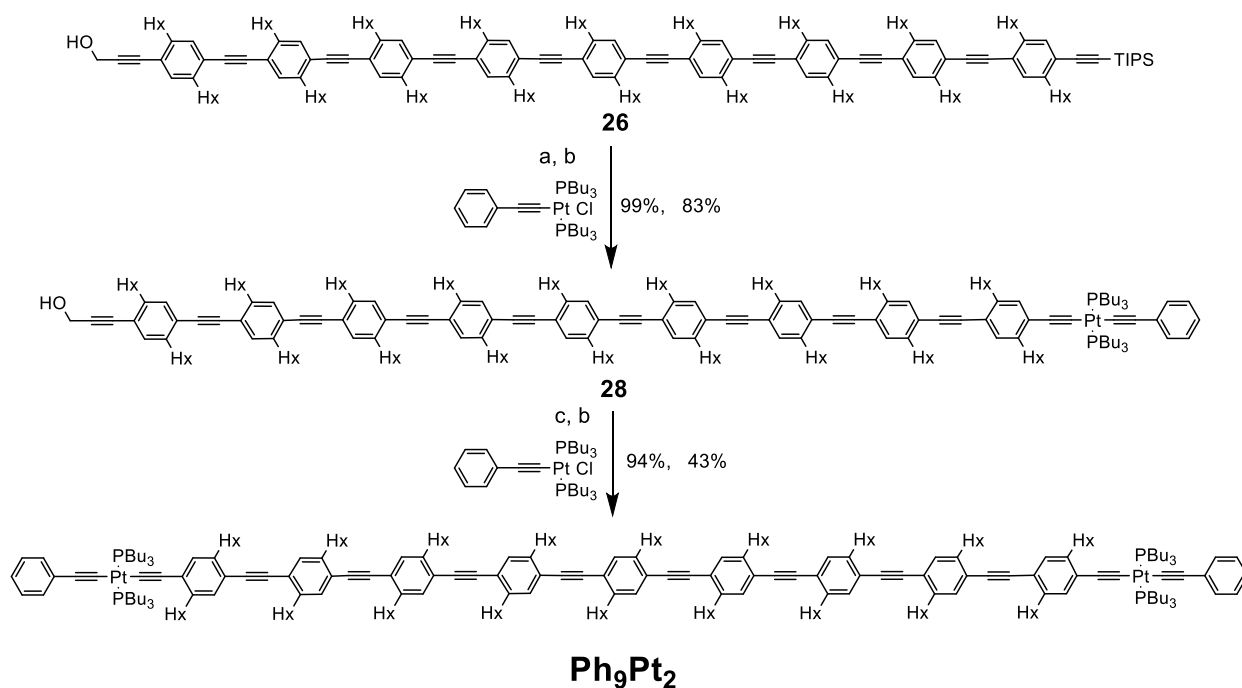
Scheme 3. Synthesis of Ph_4Pt_2

To this point, Sonogashira coupling of an aryl iodide with a free acetylene has been relatively clean with the use of $Pd(PPh_3)_2Cl_2/CuI$, as homocoupling of the free acetylene toward dimer formation was minimal (with sufficient degassing). Unfortunately, as the organic oligomers become longer, their sensitivity towards oxidative dimerization increases. For the preparation of Ph_9Pt_2 , a more active catalyst system was employed to prevent oxidative coupling of the acetylenes, $Pd_2(dba)_3/CuI/PPh_3$. Pentamer **22** (Scheme S-4) and nonamer **26** (Scheme 4 and Scheme S-5) were both prepared under these conditions. Once again, stepwise deprotection/Hagihara

couplings of each end of the known nonamer **26** with **5** afforded **Ph₉Pt₂** as a yellow, paint-like solid in 43% yield (Scheme 4).

The final Ph_nPt₂ oligomers were all characterized by ¹H and ³¹P NMR spectroscopy, as well as an analytical method. Attaining the molecular ion of all the oligomers proved to be challenging due to the high molecular weights as well as the difficulty of ionization using different methods. When successful, APCI-HRMS data is reported in the experimental method section (**Ph₁Pt₂** and **Ph₄Pt₂**). The MALDI-TOF MS were also attempted but failed; therefore, oligomers **Ph₂Pt₂** and **Ph₉Pt₂** were characterized by elemental analysis.

The ³¹P NMR spectra revealed a pattern of three resonances for each final oligomer centered at δ ~4.5 ppm; each exhibited a weak “doublet” with *J* ~2360 Hz characteristic of the ¹⁹⁵Pt-³¹P coupling, and a central resonance due to the PtP₂ units with NMR inactive Pt isotopes. The *trans* stereochemistry of the PtP₂ units was confirmed by the magnitude of the ¹⁹⁵Pt-³¹P coupling constant.⁴³⁻⁴⁵



a) TBAF, THF, 2h, dark, rt; b) CuI, NHEt₂/THF, rt, 3h; c) MnO₂/KOH, ether, dark, rt.

Scheme 4. Synthesis of Ph₉Pt₂

UV-Visible Absorption Spectroscopy. Table 1 lists a summary of the photophysical data collected for the Ph_nPt₂ oligomers. The absorption spectra for the series in THF solutions are shown in Figure 1. The S₀ → S₁ absorption maxima span over ca. 0.3 eV range from 355 to 390 nm; these transitions arise from long axis polarized π,π* transitions with some metal-to-ligand charge transfer (MLCT) character.^{16,32,44-47} (Higher energy, short axis transitions remain fairly consistent throughout the series). The molar absorptivity for each of the compounds were measured (Table 1); the trend displays an increase with spacer length⁴⁸ throughout the series.

Table 1. Summary of spectroscopic data for Ph_nPt₂ series.

n	E _{abs, max} (eV)	ε (M ⁻¹ cm ⁻¹)	E _{F, max} (eV)	φ _F (%)	τ _{F, av} (ns)	E _{P, max} (eV)	φ _P (%)	E _{TA, max} (eV)	τ _T (μs)	ε _T ^a (M ⁻¹ cm ⁻¹)
1	3.49	67,500	3.12	0.2	0.001	2.41	2.6	1.88	6.0	47,000

2	3.44	92,000	3.07	0.1	0.036	2.21	0.8	1.95	15.1	100,000
4	3.23	115,000	2.92	0.2	0.111	2.11	0.3	1.66	26.0	217,000
9	3.18	161,000	2.92	2.2	0.179	2.11	<0.1	1.66	32.9	-- ^b

^a Determined by relative actinometry using benzophenone as standard. Assume unit triplet yield for Ph_nPt₂.

^b Transient absorption response was non-linear with increasing laser energy.

The shortest oligomer **Ph₁Pt₂** exhibits the most blue-shifted absorption maximum at 355 nm which is red-shifted to 360 nm for **Ph₂Pt₂**. The spectrum for this oligomer exhibits more fine structure than the others in the series, featuring another strong absorption at a slightly lower energy (*ca.* 390 nm). Both the **Ph₄Pt₂** and **Ph₉Pt₂** oligomers display further red-shifts to 384 and 390 nm, respectively. The spectra of these larger compounds are slightly broader and less defined, and the change in absorption maximum is not significant considering the change in the length of the spacer.

The red-shift of the absorbance implies an increase in the π -electron delocalization.²⁹ In general, the absorption maxima for the Ph_nPt₂ series are all red-shifted compared to the analogous organic OPEs reported by Godt *et al.*,³⁶ suggesting that the incorporation of platinum has a direct effect on the electronic structure and conjugation length due to d, π orbital mixing of the OPEs with the platinum centers. The shapes of the spectra remain similar to their organic analogues, however. The effective conjugation length of the ground state chromophore seems to have nearly reached its limit in **Ph₉Pt₂**, as the change in absorption energy from the n = 4 oligomer is relatively small.

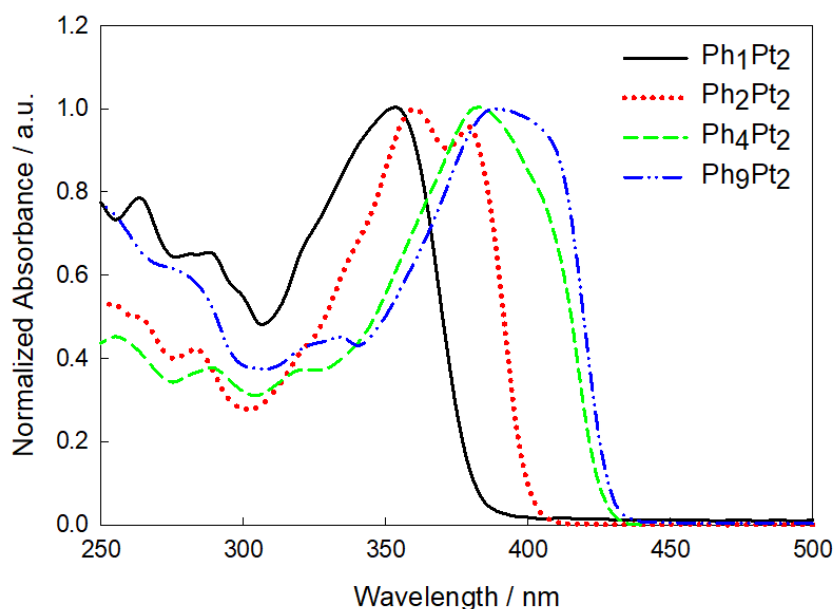


Figure 1. Normalized UV-visible absorption spectra for **Ph_nPt₂** series in THF solution.

Theoretical calculations of the highest occupied molecular orbital (HOMO) and lowest unoccupied molecular orbital (LUMO) for similar compounds have provided insight into these electronic transitions,^{34,49} finding that the combination of the platinum d orbital and the alkynyl π orbitals contributes to the HOMO, while the LUMO consists of only π^* orbitals with no contribution from the platinum d orbitals.

Emission Spectroscopy. Steady state photoluminescence (PL) spectra of the oligomer series were recorded in THF at room temperature (Figure 2). The spectra feature fluorescence between 400 – 450 nm (weak for Ph₁Pt₂

and Ph_2Pt_2) and phosphorescence between 550 – 600 nm. The fluorescence emission maxima exhibit a red-shift with the extension of the spacer length over a similar range as the ground state absorption (*ca.* 0.3 eV). The fluorescence of the series demonstrate a larger Stokes shift (~ 0.3 eV) than for the Pt_n series reported by Liu *et al.*,²² but it is fairly consistent with the analogous organic series measured by Godt,³⁶ as is the general shape of emission. The fluorescence is relatively weak for the $n = 1, 2$ and 4 oligomers ($\phi_F \sim 0.2\%$), but the quantum yield of the $S_1 \rightarrow S_0$ radiative transition increases by an order of magnitude for Ph_9Pt_2 (Table 1). The energy of the fluorescence changes very little from Ph_4Pt_2 (424 nm) to Ph_9Pt_2 , (425 nm).

The fluorescence energies continually decrease (red-shift of λ_{em}) with increase in oligomer length which suggests that the singlet exciton is delocalized across the π -electron system for $n = 1, 2$ and 4, and these energies are red-shifted in comparison with the organic analogues previously reported.³⁶ However, the fluorescence emission from Ph_9Pt_2 is almost identical to the analogous organic OPE nonamer reported by Godt.³⁶ This suggests that the singlet exciton is confined to the OPE oligomer and does not extend into the Pt centers, and implies that the any increase in conjugation involving d, π^* mixing in the Ph_nPt_2 series has been reached by $n = 4$. The low yields of fluorescence in the emission spectra for the series indicates that intersystem crossing dominates decay of the singlet excited state. For other platinum-acetylide oligomers, the reported ISC quantum yields approach unity.⁵⁰⁻⁵¹ It is apparent from the data herein, however, that as the percent heavy metal character decreases in relation to the overall π framework, the rate of ISC decreases.

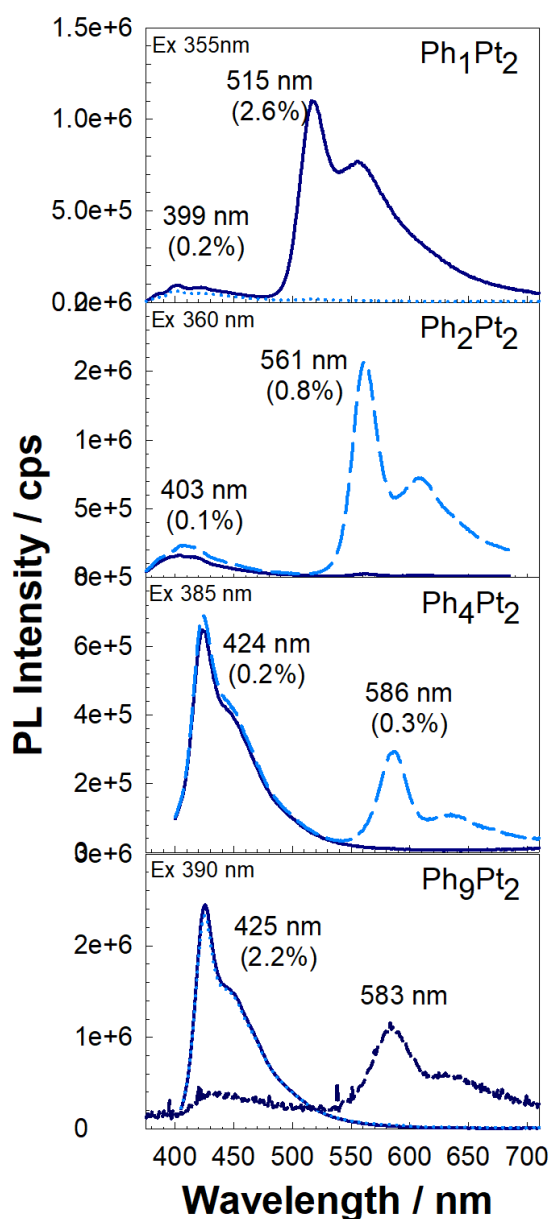


Figure 2. Steady state photoluminescence spectra of the Ph_nPt₂ series in THF solution. Solid lines for air saturated solutions (except Ph₁Pt₂, which is argon outgassed). Dashed lines are argon outgassed solutions. Peak wavelengths for the fluorescence (399 – 425 nm) and phosphorescence (515 – 586 nm) are indicated in the plots. Numbers in parenthesis are the fluorescence and phosphorescence quantum yields. Note that the phosphorescence of Ph₉Pt₂ was too weak to detect with steady-state emission. The phosphorescence spectrum shown was obtained by detection with gated/intensified CCD following 355 nm pulsed excitation.

Fluorescence lifetime data is summarized in Table 1. Within the series, the lifetime of the singlet excited state increases along with oligomer length. This trend is consistent with the premise that as the excited state becomes more π^* character and less d-orbital character from the heavy Pt-atoms, the rate of ISC is lowered; thus, the decay rate of the singlet excited state decreases (it becomes longer-lived).

The argon-degassed samples revealed lower energy phosphorescence emission at 515, 561, 586, and 583 nm in oligomers **Ph₁Pt₂**, **Ph₂Pt₂**, **Ph₄Pt₂**, and **Ph₉Pt₂**, respectively (Figure 2). At room temperature, the phosphorescence emission was generally broad, lacking significant vibronic structure. As the oligomer length increased in the series, the emission maximum red-shifted and the quantum yield decreased (2.6 to <0.1%), and

very weak emission from the triplet detected in **Ph₉Pt₂** at room temperature in the steady-state experiments. The low phosphorescence quantum yield of **Ph₉Pt₂** reflects the lower Pt-metal contribution compared to the organic part in this oligomer which leads to lower ISC yields; as well as lower rates of radiative decay. The triplet energy of **Ph₉Pt₂** oligomer is roughly the same as the triplet energy of **Ph₄Pt₂** oligomer, indicating the extent of delocalization of the triplet in the series has reached its limit in **Ph₄Pt₂**; it suggests that the triplet exciton is most likely ligand-based in the nonamer, while the tetramer may include some d-character via delocalization across the Pt-atoms.

The phosphorescence emission in dinuclear platinum compounds is generally characterized as originating from the π, π^* ligand-based triplet state,⁵² even though population of T₁ occurs via efficient spin-orbit coupling⁵³ between the excited organic ligands and the heavy metal platinum atom⁵⁴. Emission from this state is not typically seen at room temperature for strictly organic OPEs. However, low temperature studies of similar monomers and polymers,⁵⁵ as well theoretical calculations of similar oligomer structures,⁵³ give insight into the energies of the triplet states in similar organic structures for comparison with the dinuclear platinum series herein. Photoluminescence experiments of poly(phenylene ethynylene) films at 80 K reveal triplet energies around 1.9 eV;⁵⁵ these values most likely correlate to the highest degree of delocalization within the $^3\pi, \pi^*$ exciton in PPEs. Similarly, quantum chemical calculations of OPEs suggest similar lowest triplet energies in oligomers greater than n = 10 repeat units.⁵³

Predicted T₁ energies for OPEs with 'n' repeat units were also reported⁵³, and calculated values can be compared to the E_{T1} of the platinum-capped Ph_nPt₂ series measured herein. Beljonne *et al.* estimated that the E_{S₀-T₁} for the n = 2 OPE (analogous with **Ph₂Pt₂**) would be ~2.5 eV; this is comparatively higher than the phosphorescence energy measured for **Ph₂Pt₂** (2.21 eV). Similarly, the n = 4 OPE triplet energy is calculated to be ~2.3 eV above ground state—also higher than the measured value for **Ph₄Pt₂** (2.11 eV). The differences in values decrease with the decrease in overall Pt-character in the Ph_nPt₂ molecules. The comparisons suggest that perhaps some d character does exist in the triplet exciton to further lower the energy of this state for the n = 1, 2 and 4 oligomers.

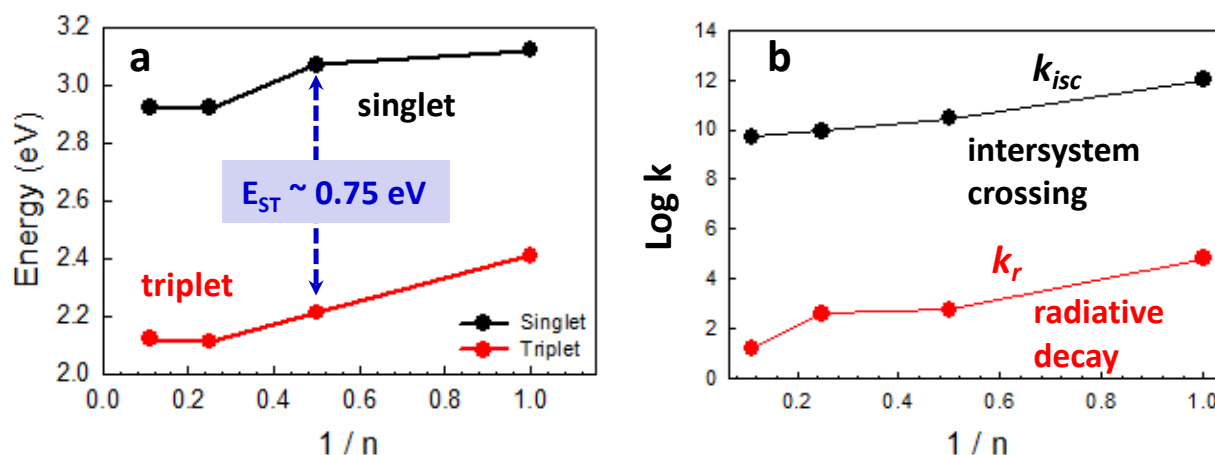


Figure 3. a) Plot of the singlet and triplet state energies for **Ph_nPt₂** series vs. 1/n where n = OPE length. Singlet and triplet energies determined from the band maxima of the fluorescence and phosphorescence spectra (Table 1). b) Plot of the intersystem crossing and triplet radiative decay rates for **Ph_nPt₂** series vs. 1/n.

Plots of the trends in the singlet and triplet state energies and the rates of intersystem crossing (k_{isc}) and triplet radiative decay (k_r) are illustrated in Figure 3 (plotted vs. 1/n where n = OPE length). The singlet and triplet

energies are derived from the maxima of the fluorescence and phosphorescence spectra (Table 1), while the rates are determined from the fluorescence lifetimes (k_{isc}) and the triplet lifetimes and phosphorescence quantum yields (k_r). First, across the series, the singlet-triplet splitting (E_{ST}) is nearly constant at ~ 0.75 eV. This splitting value is very similar to that observed for a variety of π -conjugated oligomers and polymers, and it appears to be a fundamental limit in π -conjugated electronic systems.^{23,55-56} Interestingly, we observe that both k_{isc} and k_r decrease according to a similar trend with increasing length of the OPE units. These trends are believed to arise due to a decrease in the spin-orbit coupling (SOC) effect as the oligomer length increases. A reduction in SOC is anticipated to lower the rates of both intersystem crossing and triplet radiative decay. This expectation arises because both processes involve spin transitions from triplet to singlet states, and the influence of metal-induced SOC should impact them similarly.

Transient Absorption. Transient absorption spectra for the Ph_nPt_2 series were measured in deoxygenated THF solutions and spectra collected 30 ns after excitation by 355 nm pulse (10 ns, 8 mJ pulse⁻¹). The spectra are presented in Figure 4; ΔA_{max} values, triplet lifetimes, and triplet molar extinction coefficients are summarized in Table 1.

Intense transient absorption is exhibited in the red part of the visible spectrum (550 – 800 nm) for all of the oligomers in the series. Among the series, **Ph₂Pt₂** surprisingly displays the most blue-shifted absorbance at ca. 640 nm, a 12 nm shift from **Ph₁Pt₂** (652 nm). **Ph₄Pt₂** displays a maximum absorbance at ca. 760 nm. Of all the TA spectra, **Ph₉Pt₂** exhibits the broadest absorption; the maximum is centered at ca 745 nm; however, there is a distinct broad shoulder centered around 670 nm as well.

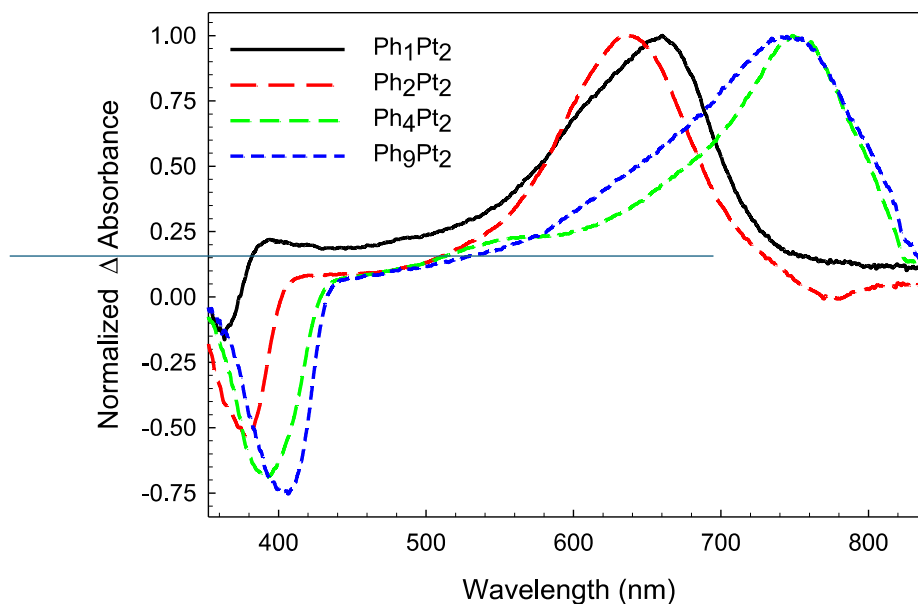


Figure 4. Transient absorption spectra of Ph_nPt_2 series measured in deoxygenated THF. Excitation at 355 nm (5 ns pulsewidth) and spectra acquired at 30 ns delay after excitation.

The triplet state lifetimes (Table 1) were determined from transient absorption decays⁵⁷. **Ph₁Pt₂** exhibits the shortest-lived triplet excited state (6.0 μs), followed by **Ph₂Pt₂** (15.1 μs) and **Ph₄Pt₂** (26.0 μs). **Ph₉Pt₂** displayed the longest-lived triplet state lifetime at 33.0 μs . The general trend is that the lifetime of the triplet exciton increases as the length of the organic spacer increases (and the contribution of the metal decreases).

The triplet molar extinction coefficients were determined using relative actinometry with benzophenone as the actinometer (Table 1). It is evident that the triplet absorptivity increases with oligomer length, reaching $> 2 \times 10^5 \text{ M}^{-1}\text{cm}^{-1}$ for **Ph₄Pt₂**. The blue-shift in the transient absorption maximum between dinuclear platinum oligomers **Ph₁Pt₂** and **Ph₂Pt₂** is rather intriguing. A similar phenomenon has been reported for a related dinuclear Pt series,⁴⁰ which involved TA differences between a phenylene-ethynylene (P) and a biphenylene-ethynylene (BP) moiety where the BP spacer was suggested to have an orthogonal-type structure with a ground state dihedral angle of 40°. ³¹ Due to the bulky hexyl side chains in the Ph_nPt₂ series, a similar phenomenon may exist (that is perhaps most evident in the dimer) even though the phenylene units in this case are further spatially separated by an ethynyl linker. The idea that the central phenyl rings in the dimer-are twisted, which disrupts the conjugation, could be plausible; this could also explain oddities in the triplet lifetime of this oligomer, but because the exact conjugation length is not known for the Ph_nPt₂ series, it is not possible to determine trends based purely on conjugation length. The apparent blue-shift between the n = 4 and n = 9 oligomers is not as surprising, as the nonamer does display a very broad absorption spectrum in relation to the tetramer, suggesting multiple geometries of the excited T_n state exist in the longer oligomer. Based on the spectral data, we believe that the conjugation length of this excited triplet state has reached its limit for n ~ 4.

Summary and Conclusions

A series of platinum end-capped phenylene-ethynylene oligomers, Ph_nPt₂ were synthesized via an iterative-convergent route described by Godt *et al*³⁶ incorporating the use of orthogonal protecting groups to produce a variety of intermediate synthons. The molecules consisted of various sized OPE units (n = 1, 2, 4 and 9) spanning two *trans*-Pt(PBu₃)₂(-C≡C-Ph) groups; the compounds were designed to characterize the influence of the heavy metal Pt atoms on the organic systems.

In comparison with the organic analogues previously reported,³⁶ it was shown that the introduction of Pt in these systems affected the ground state absorption energies throughout the series, in which d,π-mixing was suggested to cause bathochromic shift within the oligomers. The singlet excited state was also shown to be affected by the introduction of the Pt end groups; red-shifts of fluorescence emissions were noted for oligomers n = 1-4, while the singlet exciton was proposed to be mainly ligand-based in the nonamer. The fluorescence lifetimes of the oligomers were characterized, concluding that as the contribution of Pt vs. organic spacer decreased, the lifetimes of the singlet state increased, owing to less decay via ISC. The conclusion from the data was that the singlet ground and excited state were delocalized throughout the series; however, the extent of delocalization in these states seemed to be reaching its limits.

Phosphorescence energies decreased (and a decrease in quantum efficiency) with an increase in spacer length for n = 1-4 oligomers, but no phosphorescence emission was measured for the nonamer in steady state experiments, as the quantum yield of this state was too low to detect vs. the fluorescence emission. Gated fluorescence experiments of the nonamer revealed very weak phosphorescence at the same energy as the tetramer, suggesting the extent of triplet exciton delocalization had been reached by n = 4. Population of the triplet state was also apparent in all oligomers, as all compounds exhibited broad transient absorptions. The general trend for T_n delocalization was similar to other states: an increase in organic spacer implied an increased conjugation length of the exciton. The data suggested that extent of delocalization of this state had been reached as well.

Experimental Section

Materials. All solvents and chemicals used for synthesis of the platinum acetylide oligomers were reagent grade and used without further purification. Silica gel (Silicycle Inc., 230-400 mesh, 40-63 microns, 60 Å) was used for all flash chromatography. All silyl-acetylene starting materials were purchased from GFS Chemical; potassium tetrachloroplatinate and palladium-bis(triphenylphosphine) dichloride were purchased from Strem Chemicals; all other chemicals were purchased from Sigma-Aldrich. ^1H and ^{31}P NMR spectra were obtained on a Varian 300-MHz spectrometer using deuterated chloroform (CDCl_3) as the solvent and tetramethylsilane (TMS) as the internal reference. The synthesis of known compounds **1**,³⁷ **2**,³⁸ **5**,²² **7-11**,³⁶ **15-19**³⁶ and **24-26**³⁶ has been previously described in the literature; synthesis and characterization of all intermediate compounds is reported in Supporting Information.

Instrumentation. Steady-state absorption spectra were recorded on a Varian Cary 100 dual-beam spectrophotometer. Corrected steady-state emission measurements were conducted on a PTI fluorescence spectrometer. Samples were degassed by argon purging for 30 min and concentrations were adjusted to produce “optically dilute” solutions (i.e., $A_{\text{max}} < 0.20$) in THF. Quantum yields were calculated using $\text{Ru}(\text{bpy})_3\text{Cl}_2$ as a known reference.³⁹

Time-resolved emission measurements were carried out on a home-built apparatus consisting of a Continuum Surelite series Nd:YAG laser as the excitation source ($\lambda = 355$ nm, 10 ns fwhm, < 1 mJ/pulse) and detection measured with a Princeton Instruments PI-MAX intensified CCD camera detector coupled to an Acton SpectraPro 150 spectrograph. The camera delay was set to 150 ns, and the gate set to 10 ns. The spectrum was recorded as an average of 500 images. The signal was relatively low, therefore the slit to the CCD was opened up (> 50 microns) until emission was detected. Samples were degassed in THF for 45 minutes with argon in a longneck fluorescence cell.

Transient absorption measurements were conducted on a home-built apparatus,⁴⁰ which used a Nd:YAG laser for excitation and PI-Max intensified CCD camera coupled with spectrograph as a detector. Sample concentration were adjusted so that $A_{355\text{ nm}} \approx 0.8$. Triplet lifetimes were calculated using TA decay data via single exponential global fitting parameters in the SpecFit analysis software.

Relative actinometry experiments for the determination of the triplet molar extinction coefficients⁴¹⁻⁴² were conducted on a home-built transient absorption apparatus using a Nd:YAG laser for excitation and a PMT as the detector. Fine attenuation of the laser energy was achieved by use of a variable beam splitter to achieve an excitation energy range of $I = 0 - 500$ $\mu\text{J/pulse}$. Sample solutions were prepared in spectroscopy-grade benzene with matched optical densities of 0.60 at 355 nm.

Fluorescence lifetimes were obtained using the time correlated single photon counting technique (TCSPC) with a PicoQuant FluoTime 100 compact fluorescence lifetime spectrophotometer. Excitation was achieved using a UV pulsed diode laser ($\lambda_{\text{max}} 375$ nm, $P < 10$ mW). The laser was pulsed using an external BK Precision 4011A 5 MHz function generator. Decays were obtained using biexponential fitting parameters within the PicoQuant PicoHarp software.

Acknowledgements

This work was supported by the Robert A. Welch Foundation through the Welch Chair at the University of Texas at San Antonio (Award AX-0045-20110629).

Supplementary Material

Experimental methods, synthetic schemes and procedures; NMR (^1H and ^{31}P) spectra and MS spectra (PDF).

References

1. Dubinina, G. G.; Price, R. S.; Abboud, K. A.; Wicks, G.; Wnuk, P.; Stepanenko, Y.; Drobizhev, M.; Rebane, A.; Schanze, K. S. *J. Am. Chem. Soc.* **2012**, *134*, 19346-19349, <https://doi.org/10.1021/ja309393c>
2. Cooper, T. M.; Krein, D. M.; Burke, A. R.; McLean, D. G.; Haley, J. E.; Slagle, J.; Monahan, J.; Fratini, A. *J. Phys. Chem. A* **2012**, *116*, 139-149, <https://doi.org/10.1021/jp203616c>
3. Li, B.; Wen, H.-M.; Wang, J.-Y.; Shi, L.-X.; Chen, Z.-N. *Inorg. Chem.* **2015**, *54*, 11511-11519. <https://doi.org/10.1021/acs.inorgchem.5b02175>
4. Haque, A.; Al-Balushi, R. A.; Al-Busaidi, I. J.; Khan, M. S.; Raithby, P. R. *Chem. Rev.* **2018**, *118*, 8474-8597. <https://doi.org/10.1021/acs.chemrev.8b00022>
5. He, W.; Livshits, M. Y.; Dickie, D. A.; Zhang, Z.; Mejiaortega, L. E.; Rack, J. J.; Wu, Q.; Qin, Y. *J. Am. Chem. Soc.* **2017**, *139*, 14109-14119, <https://doi.org/10.1021/jacs.7b05801>
6. He, W.; Livshits, M. Y.; Dickie, D. A.; Yang, J.; Quinnett, R.; Rack, J. J.; Wu, Q.; Qin, Y. *Chem. Sci.* **2016**, *7*, 5798-5804, <https://doi.org/10.1039/C6SC00513F>
7. Dragonetti, C.; Colombo, A.; Fontani, M.; Marinotto, D.; Nisic, F.; Righetto, S.; Roberto, D.; Tintori, F.; Fantacci, S. *Organometallics* **2016**, *35*, 1015-1021, <https://doi.org/10.1021/acs.organomet.6b00094>
8. Li, Y.-P.; Fan, X.-X.; Wu, Y.; Zeng, X.-C.; Wang, J.-Y.; Wei, Q.-H.; Chen, Z.-N. *J. Mater. Chem. C* **2017**, *5*, 3072-3078, <https://doi.org/10.1039/C7TC00382J>
9. Ni, J.; Kang, J.-J.; Wang, H.-H.; Gai, X.-Q.; Zhang, X.-X.; Jia, T.; Xu, L.; Pan, Y.-Z.; Zhang, J.-J. *RSC Adv.* **2015**, *5*, 65613-65617, <https://doi.org/10.1039/C5RA13987B>
10. Wang, X.; Han, Y.; Liu, Y.; Zou, G.; Gao, Z.; Wang, F. *Angew. Chem., Int. Ed. Engl.* **2017**, *56*, 12466-12470. <https://doi.org/10.1002/anie.201704294>
11. Xu, L.-J.; Zeng, X.-C.; Wang, J.-Y.; Zhang, L.-Y.; Chi, Y.; Chen, Z.-N. *ACS Appl. Mater. Interfaces* **2016**, *8*, 20251-20257, <https://doi.org/10.1021/acsami.6b06707>
12. Bullock, J. D.; Salehi, A.; Zeman, C. J.; Abboud, K. A.; So, F.; Schanze, K. S. *ACS Appl. Mater. Interfaces* **2017**, *9*, 41111-41114, <https://doi.org/10.1021/acsami.7b12107>
13. Cekli, S.; Winkel, R. W.; Schanze, K. S. *J. Phys. Chem. A* **2016**, *120*, 5512-5521, <https://doi.org/10.1021/acs.jpca.6b03977>
14. Vivas, M. G.; De Boni, L.; Cooper, T. M.; Mendonca, C. R. *J. Phys. Chem. A* **2014**, *118*, 5608-5613.

<https://doi.org/10.1021/jp503318u>

15. Rebane, A.; Drobizhev, M.; Makarov, N. S.; Wicks, G.; Wnuk, P.; Stepanenko, Y.; Haley, J. E.; Krein, D. M.; Fore, J. L.; Burke, A. R.; Slagle, J. E.; McLean, D. G.; Cooper, T. M. *J. Phys. Chem. A* **2014**, *118*, 3749.
<https://doi.org/10.1021/jp5009658>
16. Lee, C.; Zaen, R.; Park, K.-M.; Lee, K. H.; Lee, J. Y.; Kang, Y. *Organometallics* **2018**, *37*, 4639-4647.
<https://doi.org/10.1021/acs.organomet.8b00659>
17. Wu, W.; Wu, X.; Zhao, J.; Wu, M. *J. Mater. Chem. C* **2015**, *3*, 2291-2301.
<https://doi.org/10.1039/C4TC02358G>
18. Nolan, D.; Gil, B.; Murphy, F. A.; Draper, S. M. *Eur. J. Inorg. Chem.* **2011**, *2011*, 3248-3256,
<https://doi.org/10.1002/ejic.201100424>
19. Winkel, R. W.; Dubinina, G. G.; Abboud, K. A.; Schanze, K. S. *Dalton Trans.* **2014**, *43*, 17712-17720.
<https://doi.org/10.1039/C4DT01520G>
20. Beljonne, D.; Wittmann, H.; Köhler, A.; Graham, S.; Younus, M.; Lewis, J.; Raithby, P.; Khan, M.; Friend, R.; Bredas, J. J. *Chem. Phys.* **1996**, *105*, 3868-3877,
<https://doi.org/10.1063/1.472207>
21. Chawdhury, N.; Köhler, A.; Friend, R.; Wong, W.-Y.; Lewis, J.; Younus, M.; Raithby, P.; Corcoran, T.; Al-Mandhary, M.; Khan, M. *J. Chem. Phys.* **1999**, *110*, 4963-4970,
<https://doi.org/10.1063/1.478382>
22. Liu, Y.; Jiang, S. J.; Glusac, K.; Powell, D. H.; Anderson, D. F.; Schanze, K. S. *J. Am. Chem. Soc.* **2002**, *124*, 12412-12413,
<https://doi.org/10.1021/ja027639i>
23. Glusac, K.; Kose, M. E.; Jiang, H.; Schanze, K. S. *J. Phys. Chem. B* **2007**, *111*, 929-940,
<https://doi.org/10.1021/jp065892p>
24. Li, Y.; Winkel, R. W.; Weisbach, N.; Gladysz, J. A.; Schanze, K. S. *J. Phys. Chem. A* **2014**, *118*, 10333-10339.
<https://doi.org/10.1021/jp5021388>
25. Li, Y.; Köse, M. E.; Schanze, K. S. *J. Phys. Chem. B* **2013**, *117*, 9025-9033,
<https://doi.org/10.1021/jp4032173>
26. Liao, C.; Yarnell, J. E.; Glusac, K. D.; Schanze, K. S. *J. Phys. Chem. B* **2010**, *114*, 14763-14771.
<https://doi.org/10.1021/jp103531y>
27. Keller, J. M.; Schanze, K. S. *Organometallics* **2009**, *28*, 4210-4216,
<https://doi.org/10.1021/om900195p>
28. Silverman, E. E.; Cardolaccia, T.; Zhao, X.; Kim, K.-Y.; Haskins-Glusac, K.; Schanze, K. S. *Coord. Chem. Rev.* **2005**, *249*, 1491-1500,
<https://doi.org/10.1016/j.ccr.2004.11.020>
29. Rogers, J. E.; Cooper, T. M.; Fleitz, P. A.; Glass, D. J.; McLean, D. G. *J. Phys. Chem. A* **2002**, *106*, 10108-10115,
<https://doi.org/10.1021/jp021263d>
30. Cooper, T. M.; Blaudeau, J. P.; Hall, B. C.; Rogers, J. E.; McLean, D. G.; Liu, Y. L.; Toscano, J. P. *Chem. Phys. Lett.* **2004**, *400*, 239-244,
<https://doi.org/10.1016/j.cplett.2004.10.132>
31. Cooper, T. M.; McLean, D. G.; Rogers, J. E. *Chem. Phys. Lett.* **2001**, *349*, 31-36.
[https://doi.org/10.1016/S0009-2614\(01\)01161-7](https://doi.org/10.1016/S0009-2614(01)01161-7)
32. Rogers, J. E.; Hall, B. C.; Hufnagle, D. C.; Slagle, J. E.; Ault, A. P.; McLean, D. G.; Fleitz, P. A.; Cooper, T. M. *J. Chem. Phys.* **2005**, *122*, 214701-214708,

- <https://doi.org/10.1063/1.1924450>
33. Cooper, T. M.; Krein, D. M.; Burke, A. R.; McLean, D. G.; Rogers, J. E.; Slagle, J. E.; Fleitz, P. A. *J. Phys. Chem. A* **2006**, *110*, 4369-4375,
<https://doi.org/10.1021/jp056663q>
34. Cooper, T. M.; Hall, B. C.; McLean, D. G.; Rogers, J. E.; Burke, A. R.; Turnbull, K.; Weisner, A.; Fratini, A.; Liu, Y.; Schanze, K. S. *J. Phys. Chem. A* **2005**, *109*, 999-1007.
<https://doi.org/10.1021/jp046806t>
35. Cooper, T. M.; Krein, D. M.; Burke, A. R.; McLean, D. G.; Rogers, J. E.; Slagle, J. E. *J. Phys. Chem. A* **2006**, *110*, 13370-13378,
<https://doi.org/10.1021/jp0654516>
36. Kukula, H.; Veit, S.; Godt, A. *Eur. J. Org. Chem.* **1999**, 277-286,
[https://doi.org/10.1002/\(SICI\)1099-0690\(199901\)1999:1<277::AID-EJOC277>3.0.CO;2-R](https://doi.org/10.1002/(SICI)1099-0690(199901)1999:1<277::AID-EJOC277>3.0.CO;2-R)
37. Rehahn, H.; Schluter, A.-D.; Feast, W. J. *Synthesis* **1988**, *5*, 386-388,
<https://doi.org/10.1055/s-1988-27583>
38. Lulinski, P.; Skulski, L. *Bull. Chem. Soc. Jpn.* **2000**, *73*, 951-956,
<https://doi.org/10.1246/bcsj.73.951>
39. Harriman, A. *Chem. Commun.* **1977**, 777-778,
<https://doi.org/10.1039/C3977000077>
40. Farley, R. T. Photophysics of Platinum and Iridium Organometallic Materials: From Molecular Wires to Nonlinear Optics. Ph.D. Dissertation, University of Florida, Gainesville, 2007.
41. Amand, B.; Bensasson, R. *Chem. Phys. Lett.* **1975**, *34*, 44-48,
[https://doi.org/10.1016/0009-2614\(75\)80197-7](https://doi.org/10.1016/0009-2614(75)80197-7)
42. Bonneau, R.; Carmichael, I.; Hug, G. L. *Pure Appl. Chem.* **1991**, *63*, 289-300.
<https://doi.org/10.1351/pac199163020289>
43. Mather, G. G.; Pidcock, A.; Rapsey, G. J. N. *J. Chem. Soc., Dalton Trans.* **1973**, 2095-2099.
<https://doi.org/10.1039/DT9730002095>
44. Liu, Y.; Jiang, S.; Glusac, K.; Powell, D. H.; Anderson, D. F.; Schanze, K. S. *J. Am. Chem. Soc.* **2002**, *124*, 12412-12413,
<https://doi.org/10.1021/ja027639i>
45. Khan, M. S.; Al-Mandhary, M. R. A.; Al-Suti, M. K.; Al-Battashi, F. R.; Al-Saadi, S.; Ahrens, B.; Bjernemose, J. K.; Mahon, M. F.; Raithby, P. R.; Younus, M.; Chawdhury, N.; Köhler, A.; Marseglia, E. A.; Tedesco, E.; Feeder, N.; Teat, S. J. *Dalton Trans.* **2004**, 2377-2385,
<https://doi.org/10.1039/B405070C>
46. Chawdhury, N.; Köhler, A.; Friend, R.; Younus, M.; Long, N.; Raithby, P.; Lewis, J. J. M. *Macromolecules* **1998**, *31*, 722-727,
<https://doi.org/10.1021/ma971267u>
47. Sina, A. A. I.; Al-Rafia, S. I.; Ahmad, M. F.; Paul, R. K.; Islam, S. S.; Younus, M.; Raithby, P. R.; Ho, C.-L.; Lo, Y. H.; Liu, L. *J. Inorg. Organomet. Polym. Mater.* **2015**, *25*, 427-436,
<https://doi.org/10.1007/s10904-014-0071-7>
48. Farley, R. T.; Zheng, Q.; Gladysz, J. A.; Schanze, K. S. *Inorg. Chem.* **2008**, *47*, 2955-2963.
<https://doi.org/10.1021/ic701220t>
49. Emmert, L. A.; Choi, W.; Marshall, J. A.; Yang, J.; Meyer, L. A.; Brozik, J. A. *J. Phys. Chem. A* **2003**, *107*, 11340-11346,
<https://doi.org/10.1021/jp036309x>

50. Staromlynska, J.; McKay, T. J.; Bolger, J. A.; Davy, J. R. *J. Opt. Soc. Am. B* **1998**, *15*, 1731-1736.
<https://doi.org/10.1364/JOSAB.15.001731>
51. McKay, T. J.; Bolger, J. A.; Staromlynska, J.; Davy, J. R. *J. Chem. Phys.* **1998**, *108*, 5537-5541.
<https://doi.org/10.1063/1.475943>
52. Minaev, B.; Jansson, E.; Lindgren, M. *J. Chem. Phys.* **2006**, *125*, 094306,
<https://doi.org/10.1063/1.2345194>
53. Beljonne, D.; Shuai, Z.; Pourtois, G.; Bredas, J. L. *J. Phys. Chem. A* **2001**, *105*, 3899-3907.
<https://doi.org/10.1021/jp010187w>
54. Wilson, J. S.; Köhler, A.; Friend, R. H.; Al-Suti, M. K.; Al-Mandhary, M. R. A.; Khan, M. S.; Raithby, P. R. *J. Chem. Phys.* **2000**, *113*, 7627-7634,
<https://doi.org/10.1063/1.1313527>
55. Kohler, A.; Wilson, J. S.; Friend, R. H.; Al-Suti, M. K.; Khan, M. S.; Gerhard, A.; Bassler, H. *J. Chem. Phys.* **2002**, *116*, 9457-9463,
<https://doi.org/10.1063/1.1473194>
56. Walters, K. A.; Ley, K. D.; Schanze, K. S. *Chem. Commun.* **1998**, 1115-1116.
<https://doi.org/10.1039/a709064a>
57. Cekli, S.; Winkel, R. W.; Alarousu, E.; Mohammed, O. F.; Schanze, K. S. *Chem. Sci.* **2016**, *7*, 3621-3631,
<https://doi.org/10.1039/C5SC04578A>

This paper is an open access article distributed under the terms of the Creative Commons Attribution (CC BY) license (<http://creativecommons.org/licenses/by/4.0/>)